Composites Science and Technology **34** (1989) 95–111

Smooth Indentation of Orthotropic Beams

B. V. Sankar

Department of Aerospace Engineering, Mechanics and Engineering Science,
University of Florida, Gainesville, Florida 32611, USA

(Received 8 June 1987; revised version received 29 February 1988;
accepted 6 June 1988)

ABSTRACT

An approximate Green's function for surface displacements in an orthotropic beam is derived as the superposition of the half-plane solution for displacements and the beam theory deflections. The Green's function is used to formulate the integral equation for the problem of smooth contact between a rigid cylinder and a simply supported orthotropic beam. The integral equation is solved using a least-squares approximation procedure. The contact stress distribution is presented for three materials with different degrees of orthotropy. Numerical results are given for contact force–contact length and contact force–indentation relations. The effects of curvature of the deflected beam, shear deformation and length-to-thickness ratio of the beam on the contact behavior are discussed.

1 INTRODUCTION

The problem of contact between a rigid cylinder and an orthotropic beam has two important applications: flexure tests for characterizing composite materials and low-velocity foreign object impact force estimation. In three-point and four-point flexure tests, the loading fixture consists of loading noses which have finite radius of curvature. It has also been reported that the stresses in short orthotropic beams under flexure are significantly different from those derived from beam theory results.[1] So an estimation of actual contact area and the contact stresses therein is essential for meaningful interpretation of test results. In low-velocity foreign object

Composites Science and Technology 0266-3538/89/$03·50

impact problems it is assumed that the local elastodynamic effects can be approximated by static contact behavior.[2] In that case the results of contact problems find application in the computation of impact force history, and also an estimation of stress concentrations in the vicinity of impact. In some cases static indentation tests can provide information on the impact resistance of a composite laminate.[3] Hence there is a need to develop simple analytical methods to solve contact problems involving laminated composite structures. In this paper we consider the simplest composite structural element, namely an orthotropic beam.

The problem of contact between a rigid cylinder and an orthotropic beam has been previously solved by Sun and Sankar,[4] and by Keer and Ballarini.[5] The basic principle in both methods was the use of elasticity equations to describe the local behavior and of beam theory for the global behavior. In this paper it is shown that the Green's function for surface displacements in an orthotropic beam can be obtained by adding the Green's functions for an orthotropic half-plane and an orthotropic beam. Then the Green's function can be used to formulate the integral equation for the contact problem, which can be solved numerically.

Numerical examples are given for the problem of central indentation of an orthotropic beam by a rigid, smooth cylindrical indenter. The results reported are contact stress distribution beneath the indenter, contact force–contact length relations and contact force–indentation relations. The contact stress distribution is computed for beams of three materials (graphite/epoxy, glass/epoxy and boron/epoxy) with different degrees of orthotropy. The effects of shear deformation on the contact behavior are discussed by considering the graphite/epoxy beam as an example.

2 APPROXIMATE GREEN'S FUNCTION

In this section an approximate Green's function for surface displacements in an orthotropic beam is proposed, and its accuracy is demonstrated using some numerical examples. The procedure is similar to that used for the case of an isotropic beam,[6] and is based on the superposition procedure explained in Ref. 7. Consider the problem of a simply supported orthotropic beam of rectangular cross-section and unit width subjected to a concentrated force, P, as shown in Fig. 1(a). The principal material directions 1 and 2 are parallel to the x and y axes respectively. A state of plane stress parallel to the x–y plane is assumed. In the context of contact problems our interest is in determining the surface displacements, $v(x, 0)$, in the y-direction. We shall show than an approximate expression for displacements can be obtained as the superposition of the orthotropic half-plane solution for v-

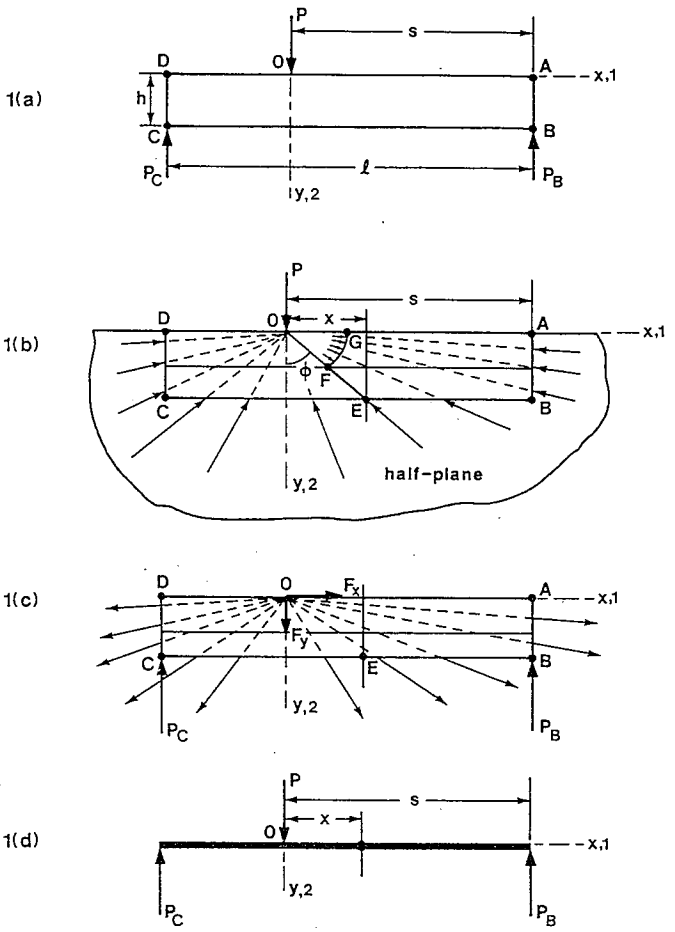

Fig. 1. Principle of superposition for calculating surface displacements in an orthotropic beam.

displacements and the beam theory deflections due to the concentrated force P, i.e.

$$v(x,0) = v_h(x,0) + v_b(x) \tag{1}$$

where v_h and v_b denote the half-plane displacements and beam theory deflections respectively.

The solution to the problem in Fig. 1(a) can be obtained as the superposition of solutions of systems shown in Fig. 1(b) and (c). The expression for surface displacements due to a concentrated force, P, in an orthotropic half-plane under plane stress can be derived as[8]

$$v_h(x,0) = -k_h P \log|x| + \text{const.} \tag{2}$$

where $k_h = (\lambda_1 + \lambda_2)/\pi E_2$, λ_1 and λ_2 being the roots of the characteristic equation

$$S_{11}\lambda^4 - (2S_{12} + S_{66})\lambda^2 + S_{22} = 0$$

where $S_{11} = 1/E_1$, $S_{22} = 1/E_2$, $S_{66} = 1/G_{12}$ and $S_{12} = -\nu_{12}/E_1$. E_1 and E_2 are the Young's moduli in the 1 and 2 directions, G_{12} is the shear modulus in the 1–2 plane and ν_{12} is the Poisson's ratio. The constant term in eqn (2) cannot be determined uniquely in half-plane problems, but it will be seen later that in contact problems we need only relative displacements, and there is no need to evaluate the constant.

The displacements, $v_{hb}(x, 0)$, of the system shown in Fig. 1(c) may be obtained from beam theory equations. The justification for using beam theory is that now the load is somewhat distributed and also the displacements are evaluated not on the loading face but on the opposite face given by $y = 0$. Further it will be shown that the displacements, v_{hb}, are approximately equal to the deflection, v_b, in a beam subjected to a concentrated force, P, as shown in Fig. 1(d). The stresses in the half-plane due to the concentrated force are[9]

$$\sigma_{rr} = \frac{-P(\lambda_1 + \lambda_2)\sqrt{S_{11}S_{22}}\cos\theta}{\pi r L(\theta)} \qquad \sigma_{\theta\theta} = \tau_{r\theta} = 0 \tag{3}$$

where

$$L(\theta) = S_{11}\sin^4\theta + (2S_{12} + S_{66})\sin^2\theta\cos^2\theta + S_{22}\cos^4\theta$$

and θ is measured counter-clockwise from the y-axis. The tensile radial tractions, t_{rr}, acting on the beam in Fig. 1(c) are equal and opposite to σ_{rr} given in eqns (3), i.e. $t_{rr} = -\sigma_{rr}$. The bending moment about the centroid at a section passing through the point E (Fig. 1(c)) can be easily calculated if we note that the radial tractions on face ABE are statically equivalent to the radial pressure over the circular arc FG of an arbitrary radius r in Fig. 1(b). The resultants of the radial tractions on face ABE are F_x and F_y acting at the origin, and they can be derived as

$$F_x = \int_{\phi}^{\pi/2} (t_{rr}\sin\theta) r\,\mathrm{d}\theta \tag{4}$$

$$F_y = \int_{\phi}^{\pi/2} (t_{rr}\cos\theta) r\,\mathrm{d}\theta \tag{5}$$

where $\phi = \tan^{-1}(x/h)$. After evaluating the integrals in eqns (4) and (5) we obtain

$$F_x = P\lambda_1\lambda_2[\ln(x^2 + \lambda_2^2h^2) - \ln(x^2 + \lambda_1^2h^2)]/2\pi(\lambda_2 - \lambda_1) \tag{6}$$

$$F_y = (P/2) - P[\lambda_1\tan^{-1}(x/\lambda_2 h) - \lambda_2\tan^{-1}(x/\lambda_1 h)]/\pi(\lambda_1 - \lambda_2) \tag{7}$$

The expression for bending moment is

$$M(x) = E_1 I \, \mathrm{d}^2 v_{hb}/\mathrm{d}x^2 = F_x h/2 - F_y x - P_B(s - x) \tag{8}$$

In eqn (8) $I = h^3/12$ and the reaction $P_B = P(1 - s/l)$. The beam deflections can be obtained by integrating eqn (8) twice.

In the numerical examples the orthotropic elastic constants were assumed to be $E_1 = 200\,\mathrm{GPa}$, $E_1/E_2 = 40$, $E_2/G_{12} = 2$, $\nu_{12} = 0{\cdot}25$ and $s = l/2$. The l/h ratio was varied from 8 to 20. The constants of integration in eqn (8) were evaluated using the conditions that $v_{hb} = 0$ at $x = l$ and $\mathrm{d}v_{hb}/\mathrm{d}x = 0$ at $x = 0$. The displacements were then compared with beam theory deflections due to the concentrated force, P, acting at $x = 0$ given by

$$v_b(x) = P(l^3 - 6lx^2 + 4x^3)/48E_1 I$$

Comparison of v_{hb} and v_b for $l/h = 10$ is given in Table 1. It may be seen that the maximum difference of about 4% occurs at the center of the beam. The error in approximating the system in Fig. 1(c) as that in Fig. 1(d) increased as the l/h ratio was decreased. For slender beams, $l/h = 20$, the maximum error was about 1%, and for $l/h = 8$ the error was about 6%. It should also be remembered that v_b is only part of the solution to which v_h, the half-plane displacements, have to be added to obtain the surface displacements. This will further reduce the error due to the approximation. Thus we have shown that the surface displacements due to a concentrated force in an orthotropic beam can be approximated as the sum of the half-plane solution for displacements and the beam theory deflections.

The above superposition procedure is, in fact, a local–global technique wherein the elasticity solution and the beam theory deflections describe the local and global behavior respectively. Numerical examples show that the lower limit of the l/h ratio is about 8 for this technique to be valid. There will be an upper limit also. If the beam is very thin, then in reality the beam behavior will dominate the local indentation behavior, but the superposition method will artificially introduce significant half-plane displacements. The

TABLE 1
Comparison of Deflections v_b and Displacements v_{hb}

x/l	$(E_1 I/Ph^3)v_b$	$(E_1 I/Ph^3)v_{hb}$	$(v_b - v_{hb})/v_b$
0·0	20·833	19·958	0·042
0·1	19·667	18·889	0·040
0·2	16·500	15·904	0·036
0·3	11·833	11·439	0·033
0·4	6·166 7	5·973 7	0·031
0·5	0·0	0·0	0·0

error is in the calculation of displacements in the system shown in Fig. 1(c) using beam theory. For thin beams the tractions, t_{rr}, on the bottom surface of the beam in Fig. 1(c) will still be concentrated around $x=0$. A better approximation can be obtained by solving the problem of surface loads on the upper half-plane, and repeating the superposition procedure until the traction concentration is sufficiently reduced to make use of beam theory for computing displacements. On the other hand, for very thin beams, beam theory itself will be good, and there will be no need for superposing elasticity solutions. In this paper we assume that the beam is sufficiently thick so that the superposition principle is applicable.

3 SMOOTH INDENTATION BY A RIGID CYLINDER

In this section we shall apply the approximate Green's function for solving the problem of contact between a rigid smooth cylinder and a simply supported orthotropic beam (see Fig. 2). The l/h ratio is assumed to be equal to 10 so that the approximate method described in the previous section will be applicable. The indenter is assumed to have a radius of curvature R, and its profile is approximated by $y=-x^2/2R$. The problem is defined as follows. For a given contact length, $2c$, find the contact stresses, $p(x)=-\sigma_{yy}$, beneath the indenter, the total contact force, P, and the amount of indentation, α, defined by

$$\alpha = v(0,0) - v(0,h) \tag{9}$$

The integral equation for $p(x)$ is

$$\int_{-c}^{+c} p(\xi) g(x,\xi)\,\mathrm{d}\xi = \Delta - (x^2/2R) \qquad |x| > c \tag{10}$$

where $g(x,\xi)$ is the Green's function for surface displacements in the orthotropic beam, which can be written as

$$g(x,\xi) = g_h(x,\xi) + g_b(x,\xi) \tag{11}$$

$$g_h(x,\xi) = -k_h \log|x-\xi| + \text{const.} \tag{12}$$

$$\begin{aligned} g_b(x,\xi) &= (l-2\xi)(l+2x)(0{\cdot}5l^2 - x^2 - \xi^2 - lx + l\xi)/24lE_1I \qquad x \le \xi \\ g_b(x,\xi) &= (l+2\xi)(l-2x)(0{\cdot}5l^2 - x^2 - \xi^2 + lx - l\xi)/24lE_1I \qquad x \ge \xi \end{aligned} \tag{13}$$

In eqn (10) Δ is the indenter displacement, which is also equal to $v(0,0)$, and can be written as

$$\Delta = \int_{-c}^{+c} p(\xi) g(0,\xi)\,\mathrm{d}\xi \tag{14}$$

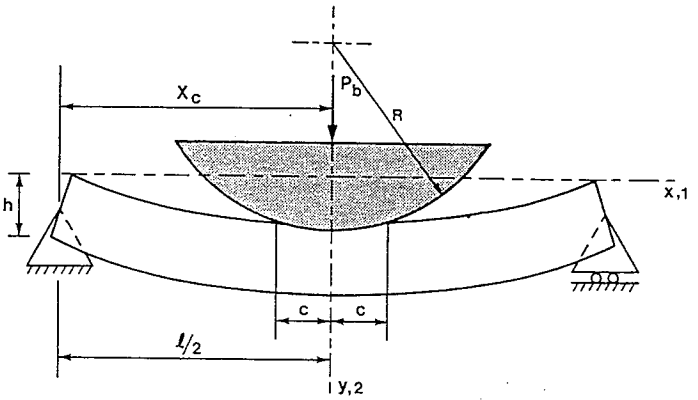

Fig. 2. Central indentation of a simply supported orthotropic beam.

From eqns (10) and (13) we obtain

$$\int_{-c}^{+c} p(\xi)[g(0,\xi)-g(x,\xi)]\,\mathrm{d}\xi = x^2/2R \qquad |x|>c \tag{15}$$

It may be noted that the constant term in eqn (12) will not appear in eqn (15).

The numerical procedure for solving the integral eqn (15) is explained below. Since the pressure distribution is symmetric about the beam center, we will only consider the region $x>0$. The pressure distribution, $p(x)$, can be assumed to be of the form

$$p(x)=\sum_{j=1}^{N_d} p_j \Pi_j(x) \tag{16}$$

where

$$\begin{aligned} \Pi_j(x)&=1 \qquad (j-1)c/N_d < x < jc/N_d \\ \Pi_j(x)&=0 \qquad (j-1)c/N_d > x > jc/N_d \end{aligned} \tag{17}$$

and N_d is an integer. The coefficients, p_j, are determined by choosing a number, N_c, of collocation points where eqn (15) is satisfied. This procedure results in a set of linear equations:

$$\sum_{j=1}^{N_d} A_{ij}p_j = x_i^2/2R \qquad i=1,\ldots,N_c \tag{18}$$

where

$$A_{ij}=\int_{-c}^{+c} \Pi_j(\xi)[g(0,\xi)-g(x_i,\xi)]\,\mathrm{d}\xi \tag{19}$$

In the numerical examples N_d was equal to 35, N_c was equal to 40, and the IMSL least-squares subroutine LLSQF was used on a VAX-11/780 computer to solve the system of eqns (18).

The total contact force, P, is given by

$$P = (2c/N_d) \sum_{j=1}^{N_d} p_j \tag{20}$$

The amount of indentation is defined as the difference between the displacement of the indenter and the displacement, $v(0, h)$ (see eqn (9)). The latter can be assumed to be equal to the beam theory deflection, $v_b(0)$. Thus

$$\alpha = v(0, 0) - v_b(0) \tag{21}$$

Such a definition of indentation has been found to be useful in low-velocity impact force calculations. From eqns (11), (14) and (21) we obtain

$$\alpha = \int_{-c}^{+c} p(\xi) g_h(0, \xi)\, d\xi \tag{22}$$

It may be noted that the Green's function, $g_h(x, \xi)$ (see eqn (12)), contains an indeterminate constant term. In order to eliminate the constant we can subtract the function $g_h(l/2, \xi)$ from $g_h(0, \xi)$ in eqn (22), since we know that $v(l/2, 0)$ is equal to zero. Thus we get the result

$$\alpha = \sum_{j=1}^{N_d} p_j \int_{-c}^{+c} \Pi_j(\xi)[g_h(0, \xi) - g_h(l/2, \xi)]\, d\xi \tag{23}$$

In evaluating the integrals in eqns (19) and (23), an expression for normal displacements on the boundary of the half-plane due to a uniform load, say p_0 over $-t < x < +t$, is needed. For the case of plane stress the relative displacements can be expressed as[10]

$$v_h(x, 0) - v_h(0, 0) = -k_h p_0 t[(1 - \bar{x}) \log|1 - \bar{x}| + (1 + \bar{x}) \log|1 + \bar{x}|] \tag{24}$$

where $\bar{x} = x/t$.

4 NUMERICAL RESULTS

In the numerical examples three orthotropic materials were used. Their elastic constants are listed in Table 2. The length of the beam is taken as 100 mm and $l/h = 10$. The width of the beam is assumed to be unity. Two indenters, $R = 3{\cdot}125$ mm and $R = 25$ mm, were used. The indenter with the

TABLE 2
Elastic Constants of Orthotropic Materials

Material	E_1 (*GPa*)	E_2/E_1	G_{12}/E_1	ν_{12}
Graphite/epoxy	200	0·025 0	0·012 5	0·25
Glass/epoxy	50	0·333 3	0·166 7	0·25
Boron/epoxy	200	0·1	0·033 3	0·3

smaller radius is typical of the loading noses used in three-point and four-point bending tests of composite specimens. The larger indenter represents the projectiles used in low-velocity impact testing of composite structures.

4.1 Contact stresses

For $R = 3{\cdot}125$ mm the calculations were performed up to $c/R = 0{\cdot}5$. The contact stress distribution was the same as the Hertzian solution for an orthotropic half-plane given by

$$p(x) = (2P/\pi c)\sqrt{1-(x/c)^2} \tag{25}$$

This is because the indenter radius is so small compared to the average radius of curvature of the deflected beam that the contact behavior is essentially that of the orthotropic half-plane.

The contact stresses for $R = 25$ mm are plotted in Figs 3–5. Similar results have been obtained previously in Ref. 4. It may be seen that for small c/h

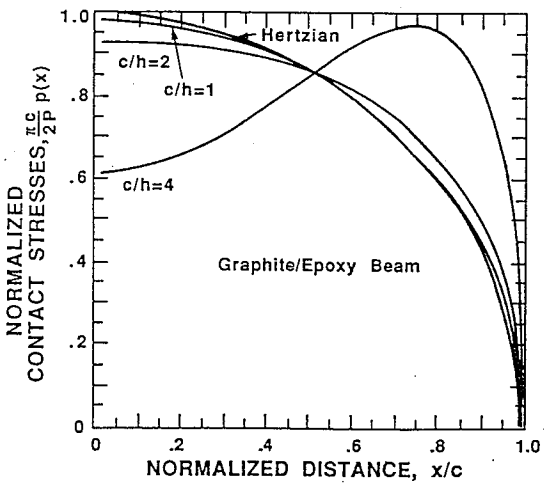

Fig. 3. Contact stresses in a graphite/epoxy beam.

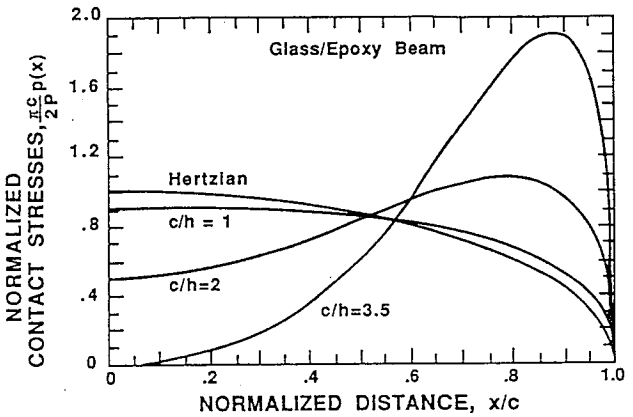

Fig. 4. Contact stresses in a glass/epoxy beam.

values the contact stress distribution in all three beams is essentially Hertzian. The severity of deviation from the half-plane solution for large c/h ratios depends on the degree of orthotropy defined by E_2/E_1. In graphite/epoxy beams (Fig. 3) the deviation from the Hertzian solution is less than that in glass/epoxy (Fig. 4). It should be noted that in glass/epoxy beams (Fig. 4) the contact stresses in the center of the contact region become zero for $c/h = 3{\cdot}5$, which indicates the impending separation of the beam from the indenter. In the case of boron/epoxy (Fig. 5) the non-dimensional contact stresses for a given c/h are intermediate between those of the other two materials. It is evident that E_1 controls the beam behavior and E_2 controls the local deformations. For smaller E_2/E_1 values local indentation dominates bending and the deviation from the Hertzian solution is small, whereas for larger E_2/E_1 the effects are opposite.

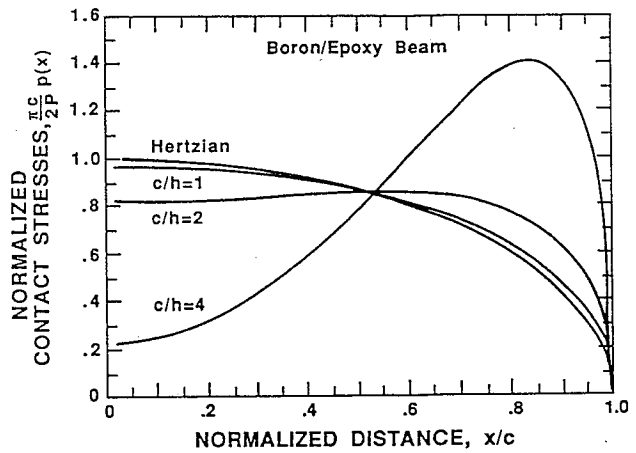

Fig. 5. Contact stresses in a boron/epoxy beam.

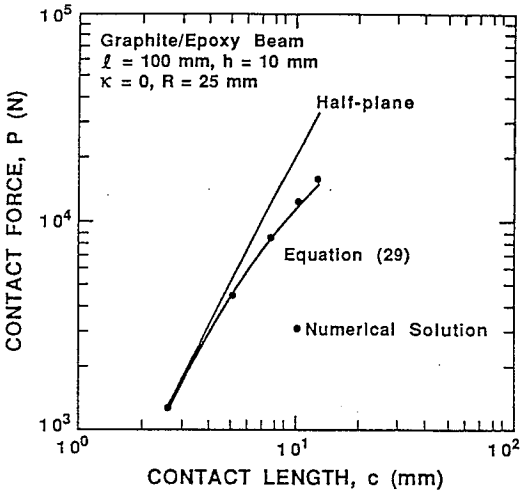

Fig. 6. Contact force–contact length relation in a graphite/epoxy beam.

4.2 Contact force–contact length relations

We shall consider the graphite/epoxy beam as an example to study the relation between the contact force and the contact length. For $R = 3{\cdot}125$ mm the P–c relations were the same as those for an orthotropic half-plane given by

$$P = k_c c^2 \tag{26}$$

where $k_c = 1/(2k_h R)$. But for the case of the larger indenter, $R = 25$ mm, the P–c relations were significantly different. Referring to Fig. 6, for $c = 10$ mm ($c/h = 1$) the contact force, P, is much less than the corresponding half-plane contact force. It may be noted that for $c/h = 1$ the contact stress distribution was almost Hertzian (Fig. 3). Now the bending of the beam has a significant effect because the radius of curvature of the beam is comparable to the indenter radius. If we consider the problem as that of two curved bodies in contact,[10] then we obtain

$$P = k_c(1 - R/R_b)c^2 \tag{27}$$

where R_b is the average beam radius at the center given by

$$R_b = 4E_1 I/Pl \tag{28}$$

Eliminating R_b from eqns (27) and (28), the P–c relation becomes

$$P = k_c c^2/(1 + \beta k_c c^2) \tag{29}$$

where $\beta = Rl/4E_1 I$. From Fig. 6 one can see that eqn (29) is a good approximation for the load–contact length relation in an orthotropic beam.

4.3 Contact law

The contact law describes the relation between the contact force and the amount of indentation. The load–indentation relation in the graphite/epoxy beam for $R = 25$ mm (filled circles) is compared with the half-plane solution in Fig. 7. In the case of half-plane the displacements cannot be determined uniquely. This difficulty was overcome by defining the indentation as

$$\alpha_h = v_h(0,0) - v_h(l/2,0) = \int_{-c}^{+c} p(\xi)[g_h(0,\xi) - g_h(l/2,\xi)]\,d\xi \tag{30}$$

where the contact pressure, $p(x)$, is given in eqn (25). Numerical integration was used to evaluate the integral in eqn (30). It was found that the load–indentation relation for the half-plane may be approximated by a power law of the type

$$P_h = k_\alpha \alpha_h^n \tag{31}$$

In order to get a closed-form expression for the contact law the integral in eqn (30) should be evaluated exactly.

For the present example the exponent n in eqn (31) was equal to 1·153 for all three materials. The contact coefficients, k_α, were 2798, 8188 and 8987 (N-mm units) for graphite, glass and boron/epoxy beams respectively. The coefficient k_α and the exponent n should be functions of beam dimensions, material elastic constants and the indenter radius, R. The contact force-indentation relation for graphite/epoxy is plotted in Fig. 7. It may be seen that the contact law of the beam is not much different from that of the half-

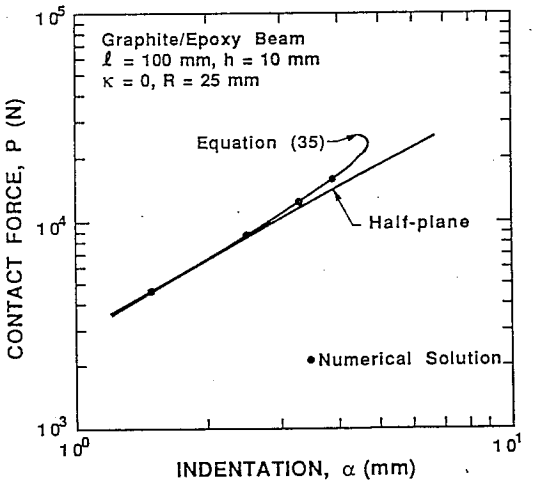

Fig. 7. Contact force–indentation relation in a graphite/epoxy beam.

plane. A more accurate expression for contact law may be obtained as explained below.

Let us assume that the contact length is small ($c/h < 1$), and that the Hertzian solution is a good approximation for contact stress distribution. Since the displacements are proportional to the load, the indentation, α_b, in the beam may be related to the half-plane indentation, α_h, as

$$\alpha_b/\alpha_h = P_b/P_h \qquad c = \text{const.} \tag{32}$$

where P_b and P_h are the contact load in the beam and half-plane respectively. The load–contact length relations, obtained previously, are

$$P_h = k_c c^2 \tag{33}$$

$$P_b = k_c c^2/(1 + \beta k_c c^2) \tag{34}$$

The load–indentation relation for a beam is obtained by eliminating P_h, α_h and c from eqns (31)–(34). The result is

$$P_b(1 - \beta P_b)^{n-1} = k_\alpha \alpha_b^n \tag{35}$$

From Fig. 7 it may be seen that eqn (35) is a better approximation for the contact law for an orthotropic beam.

It may be noted that the indentation starts decreasing as the contact force is increased (see end portion of beam indentation curve in Fig. 7). A similar behavior was also observed in the case of indentation of isotropic beams.[11] According to our definition, indentation is the difference between the center displacements at the top and bottom surfaces of the beam. As the beam radius of curvature approaches the indenter radius there is a wrapping effect which distributes the load over a larger area, thus reducing the amount of indentation. The reader is referred to Ref. 11 for further discussion on this non-unique type of load–indentation relation.

For the smaller indenter, $R = 3{\cdot}125$ mm, the beam bending effects were not significant, and the contact behavior was similar to that of the half-plane.

4.4 Shear deformation

The effect of shear deformation was considered by including the additional deflections due to shear deformation in the Green's function for the beam, $g_b(x, \xi)$. If we denote the deflection due to shear deformation as $g_s(x, \xi)$, then

$$g_s(x, \xi) = \kappa(l - 2\xi)(l + 2x)/4lG_{12}h \qquad x \le \xi$$

$$g_s(x, \xi) = \kappa(l - 2x)(l + 2\xi)/4lG_{12}h \qquad x \ge \xi$$

where κ is the shear correction factor.

A graphite/epoxy beam was considered in the numerical examples on account of its small G_{12}/E_1 ratio. κ was taken as 5/6. The shear deformations

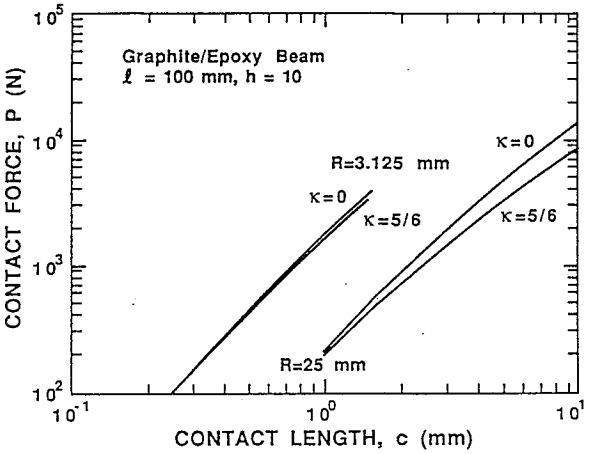

Fig. 8. Effect of shear deformation on contact length.

had no significant effect on the non-dimensional contact stresses,[12] but they had considerable effect on the contact length and indentation as shown in Figs 8 and 9. In general, inclusion of shear deformations increases the contact area for a given contact force but reduces the amount of indentation. In other words, shear deformations add to the beam bending effects. Furthermore, the effect is more pronounced in the case of the larger indenter.

4.5 Effect of beam dimensions

Another important aspect of beam indentation problems is the effect of beam dimensions relative to the indenter radius. Unfortunately all available

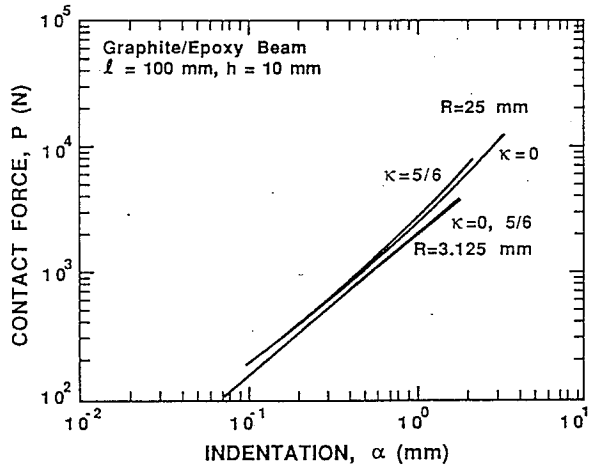

Fig. 9. Effect of shear deformation on indentation.

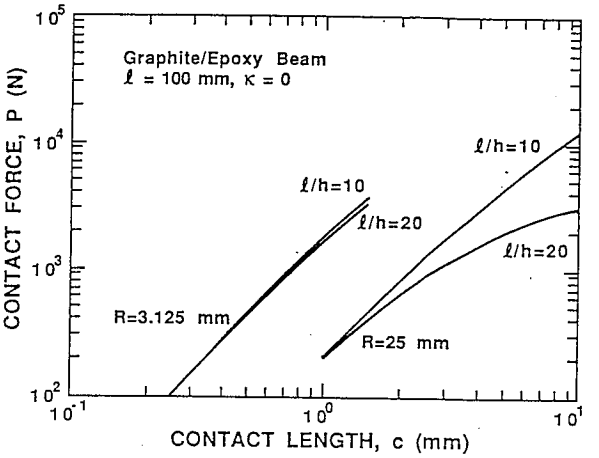

Fig. 10. Effect of l/h ratio on contact length.

studies are numerical in nature, and the role of beam dimensions on the contact behavior cannot be brought out very clearly. In this regard a closed-form solution for the integral equation (10) in terms of various beam parameters will be helpful, and this is the subject of a forthcoming paper.[13] However, the present method was used to study the contact behavior of a graphite/epoxy beam with $l/h = 20$ ($l = 100$ mm and $h = 5$ mm). The non-dimensional contact stresses did not differ significantly from those for $l/h = 10$, but the P–c and P–α relations for $l/h = 20$ plotted in Figs 10 and 11 respectively deviate from the results for the thicker beam. Obviously the reduction in thickness adds to the beam bending effects, but it is less dominant when the indenter is sharp.

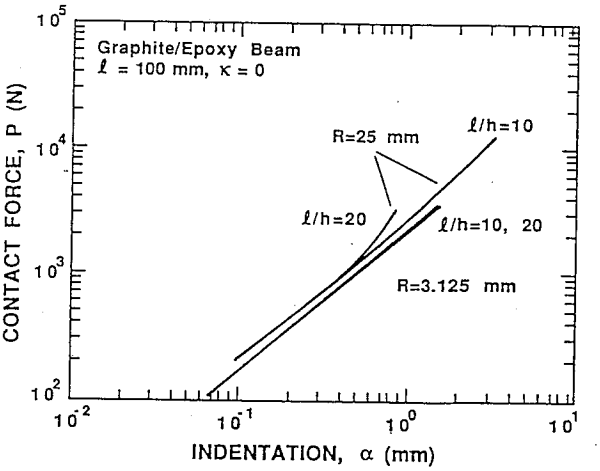

Fig. 11. Effect of l/h ratio on indentation.

5 CONCLUSIONS

A quasi-exact solution for displacements on the surface of a slender orthotropic beam ($l/h > 8$) can be obtained as the superposition of displacements in an orthotropic half-plane and beam theory deflections. This simplifies the solution procedure for contact problems. Although for small contact lengths the contact stress distribution is elliptical, the relation between contact force and contact length is affected significantly by the curvature of the deflected beam. The deviation from half-plane contact stresses for higher c/h values depends on the degree of orthotropy defined by E_2/E_1. A better formula for the load–contact length relation can be obtained by considering the problem as that of contact between two curved bodies. The curvature effect on the contact law is not very significant, but again the contact law can be modified by including the curvature of the deformed beam.

Shear deformations have no significant effect on the non-dimensional contact stresses for a given c/h ratio, but for a given contact force the contact length increases and indentation slightly reduces because of shear deformations. The effect of higher length-to-thickness ratio of the beam is similar.

Although the numerical results give a qualitative picture of contact behavior, a closed-form solution for the contact problem will be valuable in understanding the effects of various beam parameters on the contact stress distribution. Once the contact area and contact stresses therein are obtained, elasticity analysis[1] can be used to find the detailed stress field in the orthotropic beam.

ACKNOWLEDGEMENT

This work was supported by the State of Florida under the University of Florida Engineering Center of Excellence Program in New Materials, and the NASA Langley Research Center Grant NAG-1-826.

REFERENCES

1. Whitney, J. M., Elasticity analysis of orthotropic beams under concentrated loads. *Composites Sci. Techn.*, **22** (1985) 167–84.
2. Sun, C. T. & Chattopadhyay, S., Dynamic response of anisotropic laminated plates under initial stress to impact. *J. Appl. Mech.*, **42** (1975) 693–8.
3. Elber, W., Failure mechanics in low-velocity impacts on thin composite plates. *NASA TP-2152*, May 1983.

4. Sun, C. T. & Sankar, B. V., Smooth indentation of an initially stressed orthotropic beam. *Int. J. Solids Structures*, **21** (1985) 161–76.
5. Keer, L. M. & Ballarini, R., Smooth contact between a rigid indenter and an initially stressed orthotropic beam. *AIAA Journal*, **21** (1983) 1035–42.
6. Sankar, B. V., An approximate Green's function for beams and application to contact problems. *J. Appl. Mech.*, **54** (1987) 735–7.
7. Timoshenko, S. P. & Goodier, J. N., *Theory of Elasticity*, McGraw-Hill, New York, 1970, pp. 113–21.
8. Conway, H. D., The indentation of an orthotropic half-plane having inclined principal axes. *J. Appl. Mech.*, **34** (1967) 1031–2.
9. Lekhnitskii, S. G., *Theory of Elasticity of an Anisotropic Body*, Mir Publishers, Moscow, 1981, p. 153.
10. Gladwell, G. M. L., *Contact Problems in the Classical Theory of Elasticity*, Sijthoff & Noordhoff, Alphen aan den Rijn, The Netherlands, 1980, p. 51.
11. Sankar, B. V. & Sun, C. T., Indentation of a beam by a rigid cylinder. *Int. J. Solids Structures*, **19** (1983) 293–303.
12. Sankar, B. V., Contact stresses in an orthotropic beam. *Proceedings of the American Society for Composites*, Second Technical Conference, Technomic Publishing, 1987, pp. 489–99.
13. Sankar, B. V., An integral equation for the problem of smooth indentation of orthotropic beams, submitted for publication.